Research Article

Ginsenoside Rg1 suppresses cancer cell proliferation through perturbing mitotic progression

Jihee Hong [1], Dasom Gwon [1], Chang-Young Jang[*]

Research Institute of Pharmaceutical Sciences, College of Pharmacy, Sookmyung Women's University, Seoul, Republic of Korea

ARTICLE INFO

ABSTRACT

Background: Although the tumor-suppressive effects of ginsenosides in cell cycle have been well established, their pharmacological properties in mitosis have not been clarified yet. The chromosomal instability resulting from dysregulated mitotic processes is usually increased in cancer. In this study, we aimed to investigate the anticancer effects of ginsenoside Rg1 on mitotic progression in cancer.
Materials and methods: Cancer cells were treated with ginsenoside Rg1 and their morphology and intensity of different protein were analyzed using immunofluorescence microscopy. The level of proteins in chromosomes was compared through chromosomal fractionation and Western blot analyses. The location and intensity of proteins in the chromosome were confirmed through immunostaining of mitotic chromosome after spreading. The colony formation assays were conducted using various cancer cell lines.
Results: Ginsenoside Rg1 reduced cancer cell proliferation in some cancers through inducing mitotic arrest. Mechanistically, it inhibits the phosphorylation of histone H3 Thr3 (H3T3ph) mediated by Haspin kinase and concomitant recruitment of chromosomal passenger complex (CPC) to the centromere. Depletion of Aurora B at the centromere led to abnormal centromere integrity and spindle dynamics, thereby causing mitotic defects, such as increase in the width of the metaphase plate and spindle instability, resulting in delayed mitotic progression and cancer cell proliferation.
Conclusion: Ginsenoside Rg1 reduces the level of Aurora B at the centromere via perturbing Haspin kinase activity and concurrent H3T3ph. Therefore, ginsenoside Rg1 suppresses cancer cell proliferation through impeding mitotic processes, such as chromosome alignment and spindle dynamics, upon depletion of Aurora B from the centromere.
© 2021 The Korean Society of Ginseng. Publishing services by Elsevier B.V. This is an open access article under the CC BY-NC-ND license (http://creativecommons.org/licenses/by-nc-nd/4.0/).

1. Introduction

Ginsenosides, the triterpenoid saponins isolated from ginseng (*Panax ginseng* Meyer), possess medicinal properties owing to their steroidal structure and play major pharmacological roles in inflammatory responses [1], nerve growth factor activation and neuroprotective processes [2,3], cardiovascular system [4], angiogenesis [5], and diabetes and insulin metabolism [6]. Additionally, ginsenosides perturb cancer cell proliferation through expediting apoptosis, cell cycle arrest, and autophagy owing to their anticancer property [7]. Among 150 different types of ginsenosides, Rb1 and

Rg1 are the most abundant and responsible for the pharmacological properties of ginseng. Whereas ginsenoside Rg1 has been shown to increase the anticancer effect of DNA-damaging agents in hepatoblastoma [8], it also promotes the migration and proliferation of epithelial progenitor and neural stem cells [9]. Although the anticancer effect of ginsenosides Rg3 and Rg5 has been previously reported [10,11], the effect of ginsenoside Rg1 on cancer has not been clarified yet.

Eukaryote cells undergo proliferation via cell growth and division into two daughter cells through cell cycle, wherein various checkpoints monitor DNA damage, DNA replication, spindle attachment to the kinetochore (KT), and spindle orientation to ensure genome integrity [12,13]. The chromosomal passenger complex (CPC), which is composed of Inner Centromere Protein (INCENP), Borealin, Survivin, and Aurora B kinase, plays critical roles in mitotic progression, including chromosome condensation, centromere integrity, and cytokinesis [14,15]. CPC is recruited to the

* Corresponding author. Research Institute of Pharmaceutical Sciences, College of Pharmacy, Sookmyung Women's University, Seoul, 04310, Republic of Korea.
E-mail address: cyjang@sookmyung.ac.kr (C.-Y. Jang).
[1] Jihee Hong and Dasom Gwon contributed equally to this study.

chromosome arm via PRMT6-mediated histone H3 Arg2 methylation (H3R2me2a) in prophase [16], concentrated at the centromere via Haspin-mediated histone H3 Thr3 phosphorylation (H3T3ph) in prophase, and translocated to the central spindle through interacting with MKLP2 in anaphase [17]. Aurora B in CPC phosphorylates histone H3 Ser10 (H3S10ph) for chromosome condensation in prophase [18], MCAK for correction of spindle microtubules (MTs) attachment to the KTs at the centromere [19], and MgcRacGAP for contractile ring formation at the central spindle [20].

Many studies have controversially reported that ginsenoside Rg1 exerts a positive or negative effect on cell proliferation in several cell types [21–24], even though the underlying mechanisms have not been elucidated yet. In this study, we aimed to investigate the anticancer effects of Rg1 in mitosis as well as its underlying mechanisms.

2. Materials and methods

2.1. Cell culture

HeLa (uterus adenocarcinoma), MDA-MB-231 (Triple negative breast cancer), MCF7 (luminal A breast cancer), H226B (non-small cell lung carcinoma expressing wild type p53), H226Br (non-small cell lung carcinoma expressing mutant p53), H1299 (p53 deficient non-small cell lung carcinoma), A549 (lung cancer harboring wild type p53), SW480 (colorectal adenocarcinoma), HCT116 (colorectal carcinoma), and RPE1 (immortalized retinal cell) cells were cultured in Dulbecco's Modified Eagle's Medium (DMEM, Welgene), containing 10% FBS (Invitrogen), 1% penicillin, and L-glutamine (Welgene) at 37 °C supplemented with 5% CO_2. H1299 and A549 cell were cultured in Roswell Park Memorial Institute Medium (RPMI, Welgene) instead of DMEM.

2.2. Cell synchronization

HeLa S3 cells were synchronized at G1/S boundary using thymidine (2 mM, Sigma Aldrich) treatment for 18 h and released into the fresh media after washing with phosphate buffered saline (PBS, Welgene) for three times. After incubation in fresh media at 37 °C for 6 h, cells were synchronized again using nocodazole (100 ng/mL, Sigma Aldrich) treatment for 12 h and released into the fresh media after washing with PBS.

2.3. Immunofluorescence microscopy

Control and ginsenoside Rg1-treated cells were fixed with 100% methanol for 20 min and incubated at −20 °C. To observe localization of protein, cells were treated with MTSB (80 mM Pipes, pH 6.8, 1 mM $MgCl_2$, 5 mM EGTA, and 0.5% Triton X-100) for 30 s and fixed with 4% paraformaldehyde (PFA, Biosesang) for 15 min at room temperature. Next, the cells were treated with PBS-BT (PBS, 3% BSA, and 0.1% Triton x-100) for 30 min at room temperature. After incubation with primary antibodies for 30 min, the cells were washed three times with PBS-BT and treated with Alexa Fluor 594 or 488 coupled secondary antibodies (1:100) for 30 min at room temperature. To stain the chromosomes, the cells were incubated with DAPI (0.5 μg/mL) for 50–60 s and immediately washed with PBS-BT. The stained cells were mounted on slide glass using the mounting solution. The images were acquired using ZEN2 (Carl Zeiss) under a Zeiss Axiovert 200 M microscope with a 1.4 NA plan-Apo 100x oil immersion lens and a HRm CCD camera. The deconvoluted images were obtained using AutoDeblur v9.1 and AutoVisualizer v9.1 (AutoQuant Imaging). The insets show single focal planes of the boxed regions.

2.4. Chromosome fractionation

Mitotic chromosomes were isolated from nocodazole-treated mitotic cells [25]. Briefly, cells were resuspended (3.2×10^6 cells) in buffer A (10 mM HEPES, [pH 7.9], 10 mM KCl, 1.5 mM $MgCl_2$, 0.34 M sucrose, 10% glycerol, 1 mM DTT, 5 μg/mL leupeptin, 1 μg/mL pepstatin A, 1 μg/mL PMSF, 10 μg/mL aprotinin, and 0.5 μM microcyctin). Thereafter, 0.1% Triton X-100 was added, and the cells were incubated for 8 min on ice. The nuclei were pull-downed through centrifugation (4 min, 1300×g, 4 °C). After washing with buffer A, the nuclei were lysed with buffer B (3 mM EDTA, 0.2 mM EGTA, 1 mM DTT, and protease inhibitors as described above). The insoluble chromosome was collected through centrifugation (4 min, 1700×g, 4 °C) and analyzed using SDS-PAGE and immunoblotting.

2.5. Chromosome spreading

HeLa cells after Rg1 treatment were arrested in early mitosis using nocodazole (150 ng/mL) for 2 h. After mitotic-shake off, cells were treated with hypotonic solution (0.8% sodium citrate) and incubated at room temperature for 10 min. For immunostaining, cells in hypotonic solution were dropped onto the cover slip (Fisherbrand) and fixed with 2.6% PFA solution (2.6% PFA, 5 mM Sodium borate, 0.1% Triton X-100) for 15 min.

2.6. Live cell imaging

For time-lapse microscopy, HeLa cells stably expressing GFP-H2B were cultured in Leibovitz's L-15 medium (Invitrogen) supplemented with 10% FBS (Invitrogen) and 2 mM L-glutamine (Invitrogen). The cells were placed in a sealed growth chamber at 37 °C and observed using a Zeiss Axiovert 200 M microscope with a 20 × lens. The images were acquired every 3 min for 5 h using AxioVision 4.8.2 (Carl Zeiss). Thereafter, the duration of mitosis (from nuclear envelope breakdown (NEB) to anaphase onset) was measured.

2.7. Fluorescence-activated cell sorting (FACS)

The synchronized HeLa cells were fixed using 70% EtOH and extracted using 0.25% Triton X-100 in ice for 15 min. After blocking with 1% bovine serum albumin (BSA, Bioshop), cells were incubated with the primary antibody of phopho-MPM2 (Sigma Aldrich) for 1 h and Alexa Fluor 488 coupled secondary antibody (Thermo Scientific Pierce Antibodies) for 30 min at room temperature. For DNA staining, propidium iodide (PI) (20 μg/mL PI and 10 μg/mL RNase) was added and incubated for 30 min at room temperature. FACS analyses were performed using FACSCalibur (BD Bioscience) and the results were analyzed using the FlowJo_V10_CL software.

2.8. Western blot analysis

Cells were harvested and lysed in the lysis buffer (50 mM HEPES (pH 7.4), 200 mM KCl, 1 mM EGTA, 1 mM $MgCl_2$, 10% glycerol, 10% NP-40, 0.5 mM DTT, 0.5 μM microcystin, and 10 μg/mL each of leupeptin, pepstatin, aprotinin, and PMSF). For Western blot analysis, the lysates were separated through SDS-PAGE and transferred to a PVDF membrane (Millipore, Inc). The membrane was incubated with primary antibodies for overnight at 4 °C and secondary antibodies for 1 h at room temperature. Horseradish peroxidase-conjugated anti-mouse IgG (Cell Signaling Technology Inc) and anti-rabbit IgG (Enzo Inc.) were used as secondary antibodies for immunoblotting.

2.9. Chemicals and antibodies

Ginsenoside Rg1 was obtained from a commercial source (Sigma Inc.). For immunoblotting, antibodies against the following were used (Clone name, dilution, manufacturer and catalog number in brackets): H3T3ph (EP1702Y, 1:10000, Abcam, ab78351), INCENP (1:1000, Abcam, ab12183), Survivin (EP2880Y, 1:1000, Abcam, ab78351), Aurora B (H-75, 1:1000, Santa Cruz Biotechnology Inc., sc-25426), Hsp90 (4F10, 1:1000, Santa Cruz Biotechnology Inc., sc-69703), p38 MAPK (N1C3-2, 1:1000, GeneTex Inc., GTX110720), Cyclin B (H-20, 1:1000, Santa Cruz Biotechnology Inc., sc-594), Borealin (1:1000, NOVUS, NBP1-89951), histone H3 (1:10000, Cell Signaling Technology Inc., 9715), CST Anti-rabbit IgG, HRP-linked Antibody (1:2000, Cell Signaling Technology Inc., 7074S), H3S10ph (C5B11, 1:10000, Cell Signaling Technology Inc., 9649), and Goat anti-mouse IgG F(ab'')2, polyclonal antibody (HRP conjugate)(1:2000, Enzo Inc., ADI-SAB-100-J), H3R2me2a (1:1000, Merck Millipore, 07—585). MCAK (1:1000, Invitrogen, PA5-27833), Phospho-MCAK (Ser95) (1:1000, Invitrogen, PA5-38864). Unprocessed original scans of blots and gels are provided as a Source Data PDF file. For immunostaining, antibodies against the following were used (Clone name, dilution, manufacturer and catalog number in brackets): H3T3ph (EP1702Y, 1:1000, Abcam, ab78351), H3S10ph (E173, 1:500, Abcam, ab32107), INCENP (1:100, Abcam, ab12183) and Survivin (EP2880Y, 1:100, Abcam, ab78351), Aurora B (H-75, 1:100, Santa Cruz Biotechnology Inc., sc-25426), Hec1 (9G3.23, 1:100, GeneTex Inc, GTX70268), Sgo1 (1:50, Thermo Scientific Pierce Antibodies, PA5-30869), Sgo2 (1:50, Atlas Antibodies, HPA035163), β-tubulin E7 monoclonal antibody (1:100, Developmental Studies Hybridoma Bank USA, E7), Borealin (1:100, NOVUS, NBP1-89951), CREST (1:40, Antibodies Incorporated, 15-235-0001), H3R2me2a (1:1000, Merck Millipore, 07—585), H3S10ph (C5B11, 1:500, Cell Signaling Technology Inc, 9649), Alexa Fluor® 488 goat anti-rabbit IgG (1:100, Thermo Scientific Pierce Antibodies, A11034), Alexa Fluor® 594 goat anti-mouse IgG (1:100, Thermo Scientific Pierce Antibodies, A11032), Alexa Fluor® 594 goat anti-rabbit IgG (1:100, Thermo Scientific Pierce Antibodies, A11037), and Alexa Fluor® 488 goat anti-human IgG (1:100, Thermo Scientific Pierce Antibodies, A11013).

2.10. In vitro Haspin kinase assay

Active Haspin kinase (Signalchem) was used in the kinase assay. Histone H3 used as Haspin substrates was purchased from a commercial source (Signalchem). The chromatic fraction (5 μg) was incubated with 5 mM Haspin kinase and 250 mM ATP (Sigma Inc.) for 30min at 37 °C. The reaction was terminated through adding the same amount of SDS/PAGE loading buffer. The assay reaction mixtures were then separated on 15% SDS/PAGE gel and analyzed using Western blot analysis with anti-H3T3ph antibody.

2.11. Colony formation assay

The cells were seeded into petri dishes with a density of 500 cells per dish and incubated for 2 weeks. The cell culture medium was refreshed every 3 days. After 2 weeks, the cells were stained with crystal violet (0.5 mg/mL, Santa Cruz Biotechnology Inc.) for 30 min on a shaker after washing with PBS. After 30 min, the cells were washed with PBS for several times. The colonies were photographed and cell colonies with >50 cells or more were counted.

2.12. Statistical analysis

Using Student's *t*-test, the data were verified. The error bars represent the standard error (S.E.) of three independent experiments. A p value < 0.01 (two-tailed) was considered as statistically significant.

3. Results

3.1. Ginsenoside Rg1 inhibits cancer cell proliferation through delaying mitotic exit

To examine the anticancer effect of ginsenoside Rg1 in mitosis, multiple cancer cell lines, including HeLa (uterus adenocarcinoma), MDA-MB-231, MCF-7 (breast cancer cell lines), H226B, H226Br, H1299, A549 (lung cancer cell lines), SW480, and HCT116 (colon cancer cell lines), and RPE1 (normal like cell line as control) were treated with 10 μM Rg1 for the colony formation assay. Although ginsenoside Rg1 promoted cell proliferation in a normal like cell line, RPE1, and a cancer cell line, A549, the number of colonies was reduced in HeLa, MDA-MB-231, MCF-7, and H116B cell lines (Fig. 1A). This data indicated that ginsenoside Rg1 affects cell proliferation in distinctive ways in different cancer cells, which is probably based on their genetic background.

To elucidate the anti-proliferation effect of ginsenoside Rg1, the cell cycle profile of HeLa cells was examined using flow cytometry after ginsenoside Rg1 treatment. Interestingly, the number of mitotic cells increased upon Rgl treatment (Fig. 1B), indicating that it inhibits cell proliferation of HeLa cells through inducing mitotic arrest. Consistently, cyclin B1 was found to be increased in Rg1-treated cells (Fig. 1C). To determine whether ginsenoside Rg1 promotes mitotic entry or delays mitotic exit, HeLa cells were synchronized at prometaphase using thymidine-nocodazole treatment and released into the fresh media. Ginsenoside Rg1-induced mitotic arrest resulted from the delay in mitotic exit because cyclin B decreased gradually in Rg1-treated cells during the release of prometaphase cells (Fig. 1D). Time-lapse analysis of mitotic progression using HeLa cells stably expressing GFP-histone H2B exhibited that the treatment of ginsenoside Rg1 impeded chromosome alignment, leading to a lengthening of the duration from nuclear envelop breakdown to the onset of anaphase (Fig. 1E, Movie 1 and 2). Therefore, we concluded that ginsenoside Rg1 perturbs cell proliferation through delaying mitotic progression.

Supplementary video related to this article can be found at https://doi.org/10.1016/j.jgr.2021.11.004

3.2. Ginsenoside Rg1 disrupts the integrity of mitotic chromosomes and spindle fibers

To investigate the molecular mechanism underlying ginsenoside Rg1-mediated mitotic delay, HeLa cells were examined through immunostaining using antibody against β-tubulin to assess the mitotic structures, including the mitotic spindles and chromosomes. Interestingly, the width of the metaphase plate increased significantly in ginsenoside Rg1-treated cells (Fig. 2A), suggesting that it perturbs chromosomal integrity, such as chromosome condensation and centromeric cohesion during mitosis. Additionally, the intensity of mitotic spindles and the distance between the spindle poles were substantially increased due to ginsenoside Rg1 treatment (Fig. 2A and B), indicating that it also causes hyperstabilization of mitotic spindles through perturbing spindle dynamics. However, spindle MT stabilizing factors, such as HURP and Mdp3, and destabilizing factors, such as DDA3 and Kif2a, did not changed in Rg1-treated cells (Fig. 2C—F).
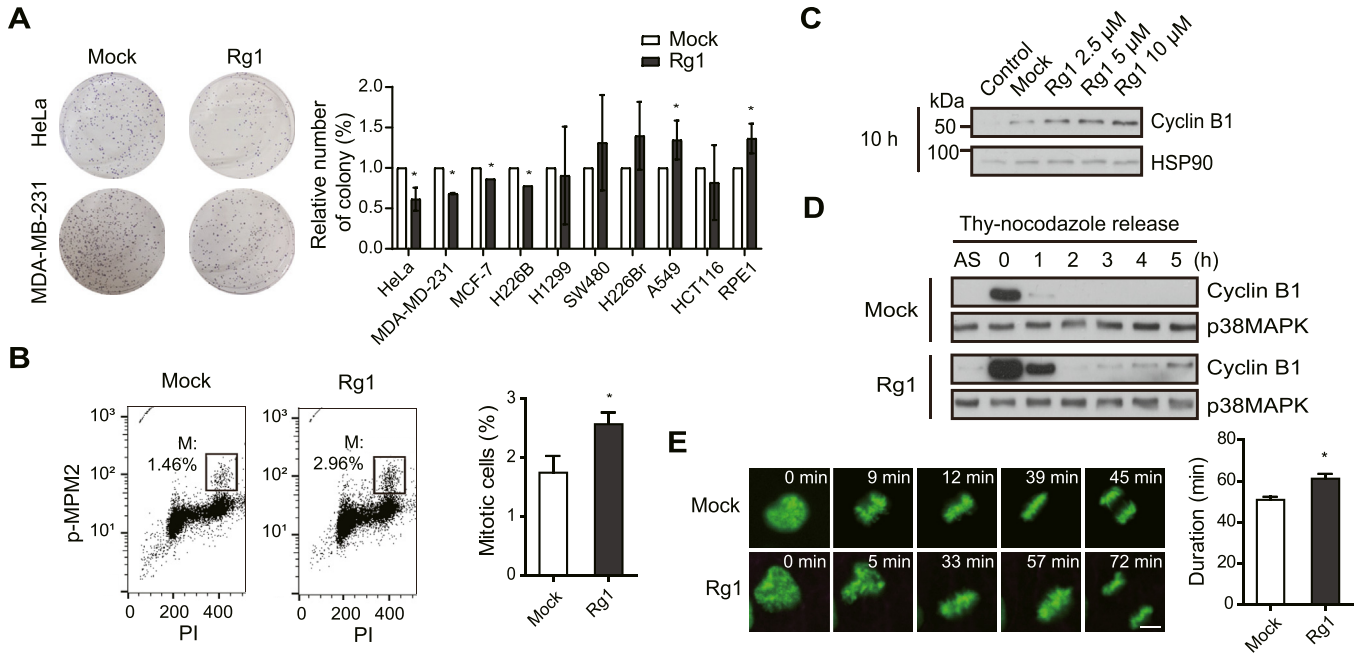
Fig. 1. Ginsenoside Rg1 delays mitotic exit. **A.** The representative images and statistical analysis of colony formation of indicated cancer cells upon ginsenoside Rg1 treatment. **B.** Ten hours post ginsenoside Rg1 treatment, HeLa cells were stained with anti-phospho-MPM2 antibody for mitotic cells and propidium iodide (PI) for DNA and analyzed using FACS. Mitotic index was plotted from three independent experiments. M, mitotic index. **C.** Ten hours post ginsenoside Rg1 treatment, HeLa cells were harvested and analyzed using the Western blot analysis with the indicated antibodies. HSP90 served as a loading control. **D.** HeLa S3 cells were synchronized with thymidine-nocodazole treatment and released into fresh media after treatment with ginsenoside Rg1 for 10 h. Cell lysates from the indicated time points were analyzed using Western blot analysis. P38MAPK served as a loading control. Thy, Thymidine. AS, unsynchronized cells. **E.** Ten hours after ginsenoside Rg1 treatment, HeLa cells expressing GFP-Histone H2B cells were imaged by time lapse. Images were captured every 3 min to monitor mitotic progression. The duration from nuclear envelop breakdown to the onset of anaphase was determined (n = 30 cells). Scale bar, 5 μm. Error bars, SEM. *p < 0.01 (two-tailed *t*-test).
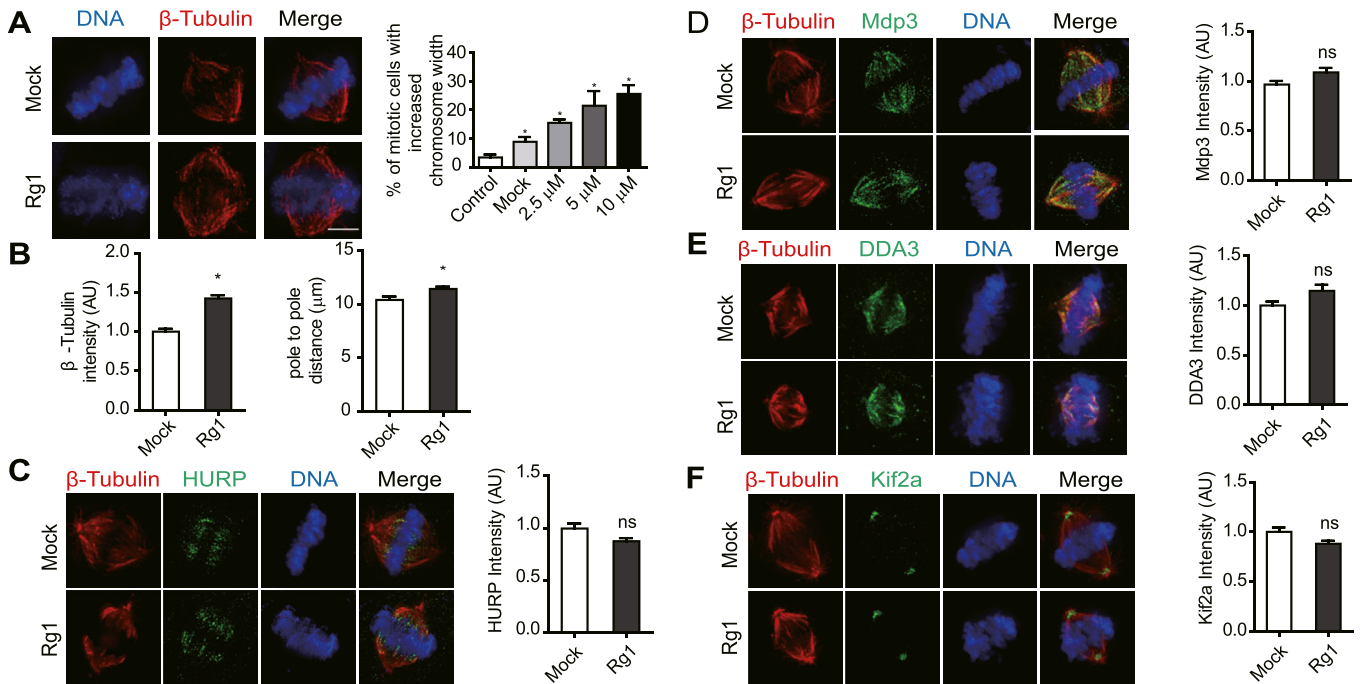

Fig. 2. Ginsenoside Rg1 disrupts spindle dynamics. **A-B.** Ten hours post ginsenoside Rg1 treatment, HeLa cells were fixed using MeOH and stained with β-tubulin and DAPI. The width of metaphase plate, intensity of spindle, and pole-to-pole distance were determined (n = 30 metaphase cells in three independent experiments). **C–F.** Ten hours after ginsenoside Rg1 treatment, HeLa cells were stained with indicated antibodies. The intensities of indicated proteins were measured and plotted (n = 30 metaphase cells in three independent experiments). AU, arbitrary units. Scale bars, 5 μm. Error bars, SEM. *p < 0.01 (two-tailed *t*-test).

Since PRMT6-mediated asymmetric methylation of histone H3 at Arg2 (H3R2me2a) recruits chromosomal passenger complex (CPC), which comprises Aurora B, Survivin, Borealin, and INCENP, to phosphorylate histone H3 at Ser10 (H3S10ph) and concomitant
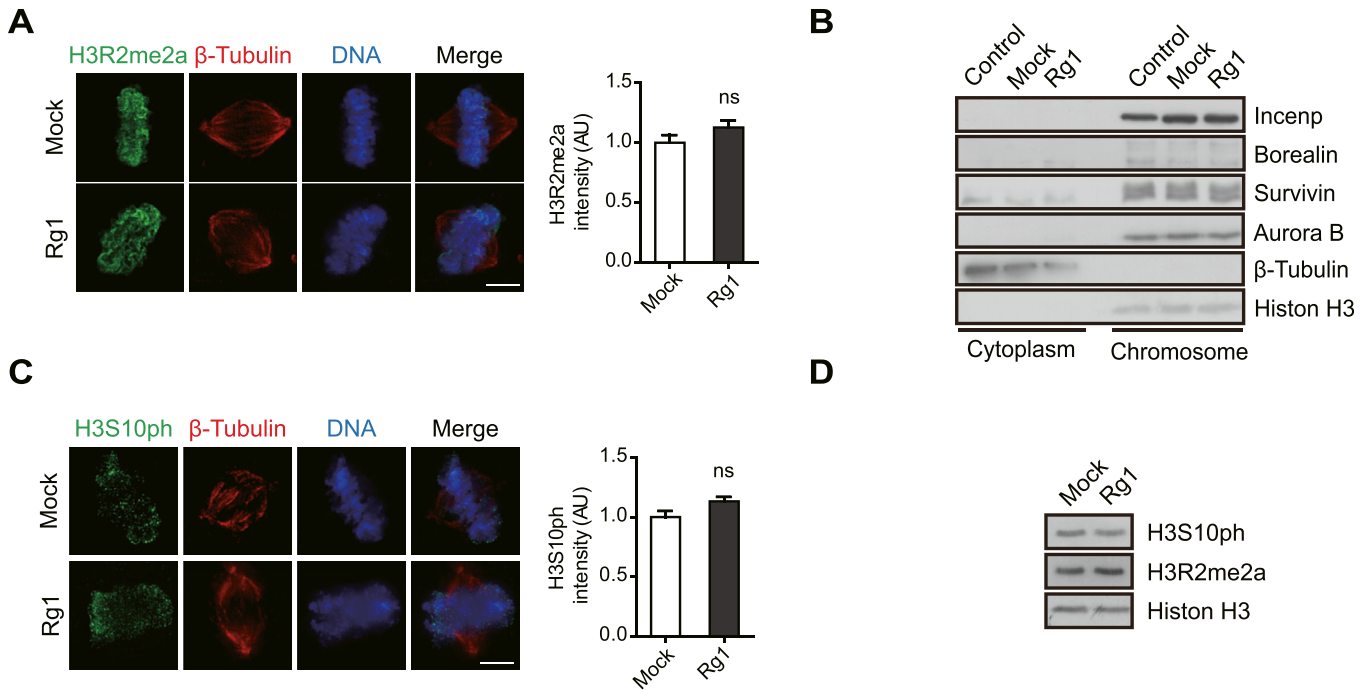
Fig. 3. Ginsenoside Rg1 disrupts chromosome condensation. **A.** Ginsenoside Rg1-treated cells were stained with the indicated antibodies and the intensity of H3R2me2a was determined and plotted (n = 30 cells from three independent experiments). **B.** Ten hours post ginsenoside Rg1 treatment, the cytosol and chromosome were fractionated from cells and analyzed using Western blot analysis with the indicated antibodies. β-Tubulin and Histone H3 served as control for fractionation. **C.** After staining the cells with the indicated antibodies, the intensity of H3S10ph was determined for ginsenoside Rg1-treated cells and plotted (n = 30 cells from three independent experiments). **D.** Chromosome fraction prepared as in (B) was analyzed using Western blot analysis with the indicated antibodies. Histone H3 served as a loading control. ns, not significant. AU, arbitrary units. Scale bars, 5 μm. Error bars, SEM. *p < 0.01 (two-tailed *t*-test).

mitotic chromosome condensation [16], we investigated whether ginsenoside Rg1 impedes H3R2me2a for Aurora B recruitment and H3S10ph for chromosome condensation. The level of H3R2me2a at the mitotic chromosomes, however, did not decrease upon ginsenoside Rg1 treatment (Fig. 3A). Accordingly, the levels of all CPC subunits in the chromosome fraction did not change upon ginsenoside Rg1 treatment (Fig. 3B). Consistent with this, the level of H3S10ph did not change upon ginsenoside Rg1-treated cells (Fig. 3C and D). Therefore, we conclude that ginsenoside Rg1 does not perturb histone modification for chromosome condensation.

3.3. Ginsenoside Rg1 disturbs targeting of CPC to centromere

To determine the reason behind the increased width of chromosome mediated by ginsenoside Rg1, we next examined the integrity of centromeric cohesion. Intriguingly, the inter-kinetochore distance, a parameter for assessing the tension between sister KTs and rigidity of centromeric chromatin, was substantially increased upon ginsenoside Rg1 treatment (Fig. 4A and B), suggesting that it perturbs the integrity of centromeric cohesion and concurrent chromosome condensation. We then examined the level of CPC, which is usually responsible for the centromeric cohesion [26]. Notably, the levels of all CPC subunits in the centromere were dramatically decreased in ginsenoside Rg1-treated cells (Fig. 4C and D), indicating that it impedes the translocation of CPC from chromosome arm to the centromere. Since Aurora B in CPC promotes MT depolymerization at the plus end through phosphorylating of MCAK [27] (Fig. 4E), a plus end MT depolymerase, it suggested that the insufficient level of Aurora B in the centromere after ginsenoside Rg1 treatment might be the reason for increased level of spindle MT.

Given Survivin in CPC recognizes phosphorylated histone H3 Thr3 (H3T3ph) as a docking site in the centromere [28], we examined the level of H3T3ph in the centromere and found a substantial decrease in H3T3ph level in ginsenoside Rg1-treated cells (Fig. 5A). Consistent with this, the level of H3T3ph was found to be decreased in the chromosome fraction extracted from ginsenoside Rg1-treated cells (Fig. 5B). Since Haspin kinase is the corresponding kinase of H3T3ph [29], we next evaluated the level of Haspin kinase in the centromere and found no significant change (Fig. 5C). Furthermore, the level of Sgo1, which is recruited to the centromere via Bub1-mediated H2AT120ph and recognized by Borealin as a docking site for CPC [30], did not change upon ginsenoside Rg1 treatment (Fig. 5D and E). These results indicate that ginsenoside Rg1 perturbs centromeric cohesion through inhibiting H3T3ph and concomitant CPC recruitment. We next examined whether ginsenoside Rg1 inhibits Haspin kinase directly or phosphorylation of H3T3 mediated by Haspin kinase in an indirect manner. Indeed, ginsenoside Rg1 slightly inhibited the phosphorylation of histone H3 at Thr3 but not to a similar extent in *in vitro* kinase assay (Fig. 5F), suggesting that it is not an inhibitor of Haspin kinase but indirectly inhibits H3T3ph. Therefore, we conclude that ginsenoside Rg1 disrupts centromeric cohesion via impeding Haspin-mediated H3T3ph and concomitant recruitment of CPC to the centromere.

3.4. Ginsenoside Rg1 inhibits H3T3ph in a genetic background-dependent manner

To delineate the reason underlying different effects of ginsenoside Rg1 in normal and cancer cells, we examined the level of H3T3ph in karyotypically stable cell line, RPE1, and did not observe a reduction in H3T3ph (Fig. 6A). This data suggests that ginsenoside
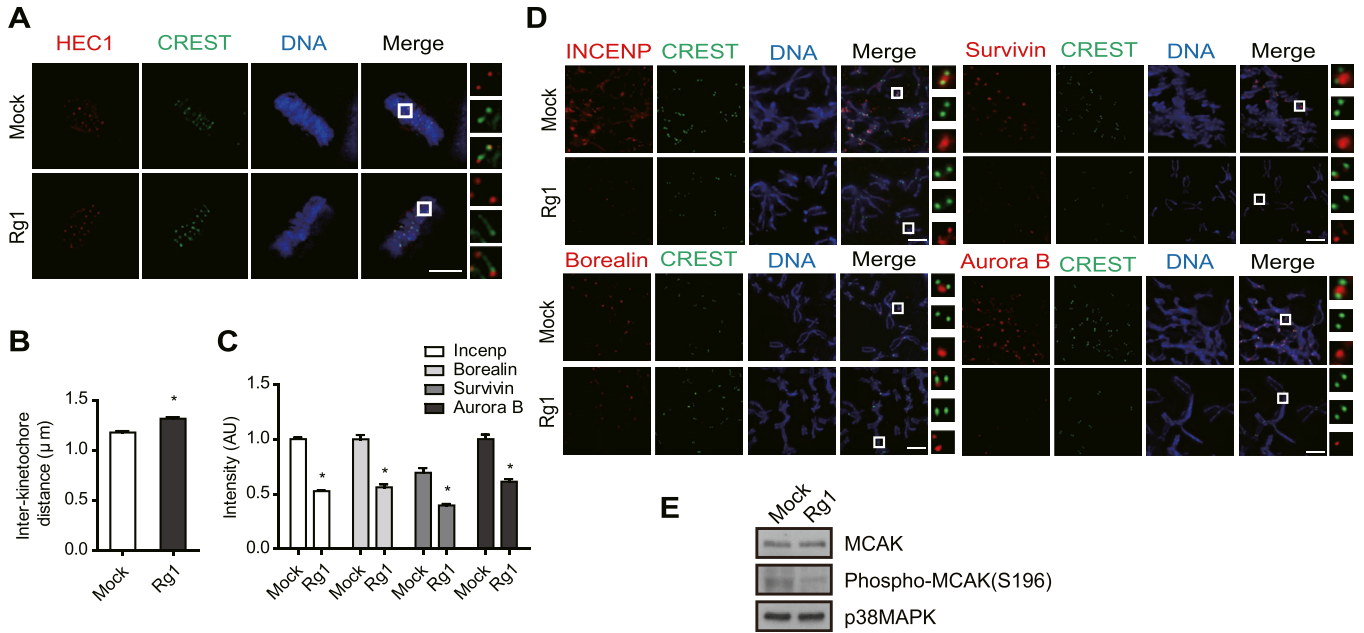
Fig. 4. Ginsenoside Rg1 perturbs centromeric cohesion. **A-B**. Ten hours post ginsenoside Rg1 treatment, HeLa cells were stained with the indicated antibodies, and the inter-KT distance was evaluated (n = 30 cells from three independent experiments). **C-D**. The intensity of CPC components was determined through immunofluorescence microscopy of HeLa chromosome spreads 10 h post ginsenoside Rg1-treatment (n = 300 centromeres from three independent experiments). **E**. The lysates from ginsenoside Rg1-treaged HeLa cells were analyzed using the Western blot analysis with the indicated antibodies. p38MAPK served as a loading control. AU, arbitrary units. Scale bars, 5 μm. Error bars, SEM. *p < 0.01 (two-tailed *t*-test).
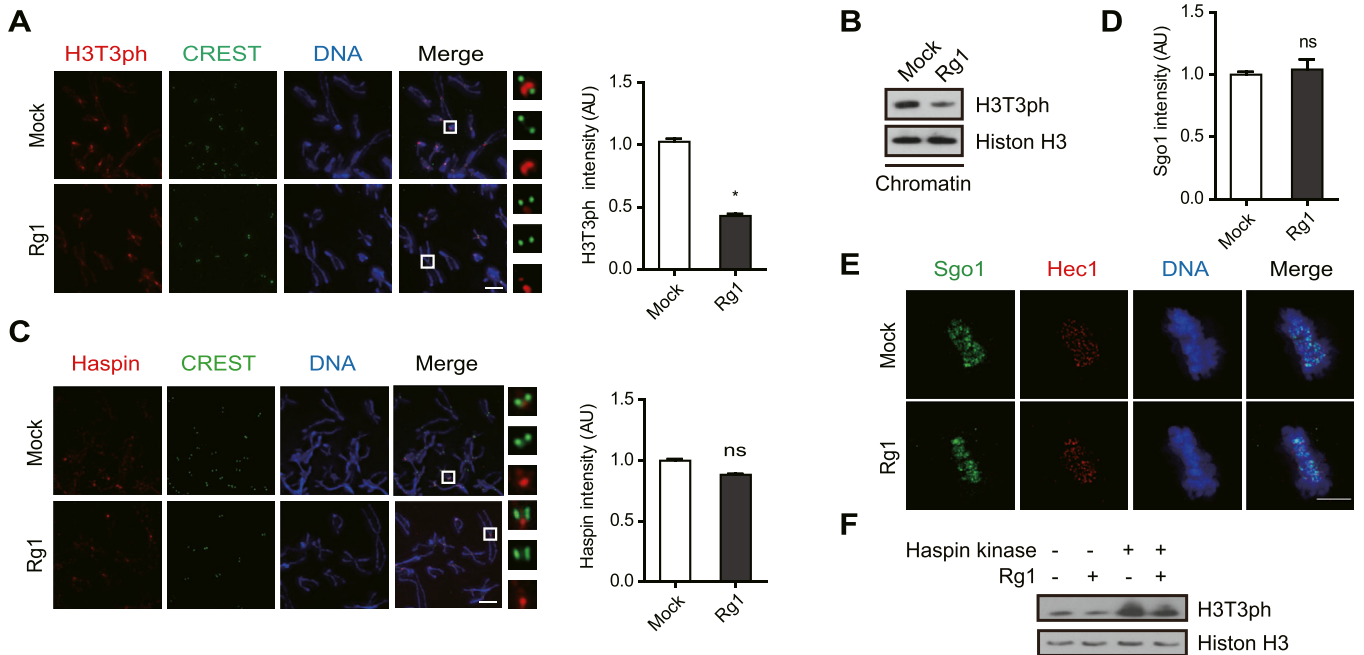

Fig. 5. Ginsenoside Rg1 impedes Haspin-mediated H3T3ph. **A-C**. Ten hours post ginsenoside Rg1 treatment, HeLa chromosome spreads were stained with the indicated antibodies. The intensity of H3T3p and Haspin was analyzed and plotted (A and C; n = 300 centromeres from three independent experiments). Alternatively, the chromosome fractions were analyzed using Western blot analysis with the indicated antibodies (B). **D-E**. The intensity of Sgo1 was analyzed from ginsenoside Rg1-treated cells and plotted (n = 30 cells from three independent experiments). **F**. Histone H3 was incubated with Haspin kinase with or without ginsenoside Rg1. The mixture of kinase assay was analyzed using Western blot analysis with the indicated antibodies. Histone H3 served as a loading control. ns, not significant. AU, arbitrary units. Scale bars, 5 μm. Error bars, SEM. *p < 0.01 (two-tailed *t*-test).

Rg1 does not affect centromeric cohesion and mitotic progression in normal cells. We next investigated the effect of ginsenoside Rg1 in MDA-MB-231, which is a triple negative breast cancer (TNBC) cell line, since it exhibited similar level of suppression of cell proliferation upon ginsenoside Rg1-treatment (Fig. 1A). As expected,

ginsenoside Rg1 inhibited H3T3ph in MDA-MB-231 cells (Fig. 6B), indicating that it inhibits Haspin-mediated H3T3ph in TNBC as observed in HeLa cells. Accordingly, the level of spindle intensity and the distance between the spindle poles were also found to be decreased upon ginsenoside Rg1 treatment in MDA-MB-231
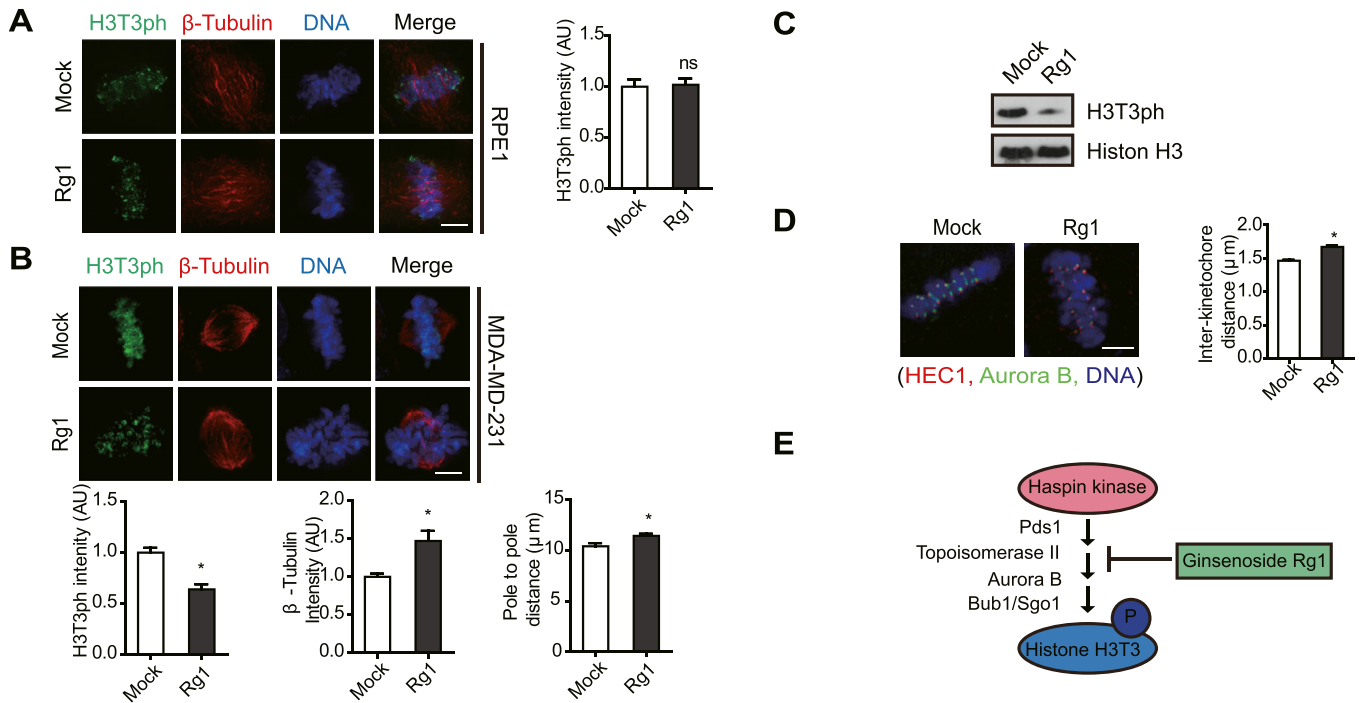
Fig. 6. Ginsenoside Rg1 induces mitotic defects in genetic background-dependent manner. **A**. The intensity of H3T3ph was analyzed from ginsenoside Rg1-treated RPE1 and plotted (n = 30 cells from three independent experiments). **B–C**. The intensity of H3T3ph and spindle, or the distance between spindle pole was analyzed from ginsenoside Rg1-treated MDA-MB-231 and plotted (n = 30 cells from three independent experiments). The cell lysate from MDA-MB-231 was analyzed by Western blot analysis using the indicated antibodies (C). Histone H3 served as a loading control. **D**. Kinetochores and centromeres were stained with antibodies against Hec1 and Aurora B, respectively. The inter-kinetochore distance was determined from ginsenoside Rg1-treated MDA-MB-231 cells and plotted (n = 300 kinetochore pairs from three independent experiments). **E**. Model for illustrating the inhibition of Haspin-mediated H3T3ph by ginsenoside Rg1. ns, not significant. AU, arbitrary units. Scale bars, 5 μm. Error bars, SEM. *p < 0.01 (two-tailed *t*-test).

(Fig. 6B and C). Also, the inter-kinetochore distance in MDA-MB 231 cells was decreased by Rg1-treatment (Fig. 6D), as in HeLa cells. Therefore, we conclude that ginsenoside Rg1 inhibits H3T3ph in HeLa and MDA-MB-231 cells but not in normal cell and other cancer cells in a genetic background-dependent manner.

4. Discussion

Although the anticancer effects of ginsenoside Rg3 have been reported in different cancer types, such as breast [31], brain [32], liver [33], and lung [34], the tumor-suppressive effect of ginsenoside Rg1 is still unclear. It has been shown that ginsenoside Rg1 sensitized hepatoblastoma to DNA-damaging agents through impairing homologous recombination repair [8], it also protected D-gal-induced liver injury in mice through inhibiting oxidative stress and DNA damage [35]. Furthermore, the effect of ginsenoside Rg1 on cell proliferation is controversial as it promotes cell proliferation and differentiation of neural stem cells through acting as a growth factor, but it inhibits the proliferation of leukemia stem cells through activating the Sirt1/TSC2 signaling pathway [9,24]. In the present study, we demonstrated that ginsenoside Rg1 promotes cell proliferation in normal as well as several cancer cells, including breast, lung, and colon cancer, but it also suppresses cell proliferation in cervical cancer and TNBC. Mechanistically, ginsenoside Rg1 perturbs mitotic progression through impeding Haspin kinase-mediated H3T3ph and concomitant enrichment of CPC in the centromere. The depletion of Aurora B, an enzymatic component of CPC, from the centromere results in the disruption of centromeric cohesion and hypo-stabilization of spindle MTs. However, the molecular mechanism underlying genetic background-dependent tumor-suppressive effect of ginsenoside Rg1 remains to be elucidated yet.

CPC plays pivotal roles in mitotic progression of various mitotic structures, including the chromosome arm in prophase, centromere in prometaphase and metaphase, central spindle in anaphase, and midbody in cytokinesis [17]. Aurora B in CPC phosphorylates different mitotic substrates at distinct locations for chromosome condensation in prophase, centromeric cohesion in metaphase, formation of cleavage furrow in anaphase, and abscission of midbody in cytokinesis. Therefore, recruiting CPC to appropriate site during mitotic processes is essential for accurate progression of mitosis. Specific histone codes such as PRMT6-mediated H3R2me2a and Haspin/Bub1-mediated H3T3ph/H2AT120ph recruit CPC to the chromosome arm in prophase and centromere in prometaphase, respectively. In this regard, the inhibition of Haspin-mediated H3T3ph by ginsenoside Rg1 might stir up mitotic defects and concurrent growth suppression.

Haspin kinase is activated through priming phosphorylation mediated by Ckd1 and concomitant phosphorylation by Plk1 to phosphorylate histone H3 at Thr 3 and generate a docking site for CPC [36]. Aurora B in CPC also phosphorylates Haspin kinase to stimulate its kinase activity for H3T3ph as CPC is also recruited by Bub1-mediated H2AT120ph and Sgo1. The centromeric localization of Haspin is dependent on its association with both the cohesin-associated protein Pds5 and sumoylated C-terminal domain of topoisomerase II [37]. The Haspin-Pds5 interaction ensures appropriate centromeric cohesion through antagonizing Wap1-mediated cohesin release in prophase since Haspin displaces and suppresses Wap1 activity. However, Aurora B/Cdk1-mediated sororin phosphorylation recruits Wap1 to the chromosome arms and removes cohesin from prophase [38]. Centromeric Sgo1 and protein phosphatase 2A (PP2A) also contribute to centromeric cohesion through preventing centromeric SA2 phosphorylation and dissociation [39]. Aurora B is also involved in regulating

centromeric cohesion through phosphorylating Sgo1 and recruiting Mps1 to KTs for promoting Sgo1 localization to the centromeres [40,41]. Therefore, the depletion of Aurora B from the centromeres mediated by ginsenoside Rg1 disrupts centromeric cohesion and results in concurrent mitotic delay (Fig. 4C and D). Although ginsenoside Rg1 clearly suppressed the phosphorylation of histone H3 at Thr3 in cells (Fig. 5A and B), it slightly inhibited H3T3ph in in vitro kinase assay (Fig. 5F). Because the localization of Haspin kinase to the centromere was not affected by Rg1-treatment (Fig. 5C), we surmise that Rg1 might directly inhibit one of proteins involved in the activation of Haspin kinase (Fig. 6E).

Conclusively, we revealed a novel tumor-suppressive effect of ginsenoside Rg1 in mitosis, which is mediated via inhibiting Haspin-mediated H3T3ph and concomitant recruitment of CPC to the centromeres. The deficiency of Aurora B activity in the centromeres perturbs centromeric cohesion and Aurora B-mediated MCAK activation, thereby inducing mitotic defects in chromosome condensation and spindle MT depolymerization, respectively. Ginsenoside Rg1-mediated mitotic defects might delay mitotic progression, thereby suppressing cancer cell proliferation.

Declaration of competing interest

No potential conflicts of interest are disclosed.

Acknowledgements

References

[1] Kim JH, Yi YS, Kim MY, Cho JY. Role of ginsenosides, the main active components of Panax ginseng, in inflammatory responses and diseases. J Ginseng Res 2017;41:435–43.

[2] Kim SK, GyuKo I, Park HJ, Chung JH, Cho KB, Kwon OY, Park KH, Ahn YS, Park CG, Kim YO. Effects of Panax ginseng on the nerve growth factor expression in testosterone induced benign prostatic hyperplasia. Saudi J Biol Sci 2018;25:66–70.

[3] Peng LL, Shen HM, Jiang ZL, Li X, Wang GH, Zhang YF, Ke KF. Inhibition of NMDA receptors underlies the neuroprotective effect of ginsenoside Rb3. Am J Chin Med 2009;37:759–70.

[4] Zhang YJ, Zhang XL, Li MH, Iqbal J, Bourantas CV, Li JJ, Su XY, Muramatsu T, Tian NL, Chen SL. The ginsenoside Rg1 prevents transverse aortic constriction-induced left ventricular hypertrophy and cardiac dysfunction by inhibiting fibrosis and enhancing angiogenesis. J Cardiovasc Pharmacol 2013;62:50–7.

[5] Chan LS, Yue PYK, Mak NK, Wong RNS. Role of MicroRNA-214 in ginsenoside-Rg1-induced angiogenesis. Eur J Pharmaceut Sci 2009;38:370–7.

[6] Yuan HD, Kim JT, Kim SH, Chung SH. Ginseng and diabetes: the evidences from in vitro, animal and human studies. J Ginseng Res 2012;36:27–39.

[7] Hong H, Baatar D, Hwang SG. Anticancer activities of ginsenosides, the main active components of ginseng. Evid-Based Compl Alt 2021;2021.

[8] Zhen N, Jin L, Ma J, Zhu JB, Gu S, Wang J, Pan QH, Ni XR, Xu M. Ginsenoside Rg1 impairs homologous recombination repair by targeting CtBP-interacting protein and sensitizes hepatoblastoma cells to DNA damage. Anti Cancer Drugs 2018;29:756–66.

[9] Gao J, Wan F, Tian M, Li YY, Li YX, Li Q, Zhang JP, Wang YX, Huang X, Zhang LJ, Si YC. Effects of ginsenoside-Rg1 on the proliferation and glial-like directed differentiation of embryonic rat cortical neural stem cells in vitro. Mol Med Rep 2017;16:8875–81.

[10] Kim SJ, Kim AK. Anti-breast cancer activity of fine black ginseng (Panax ginseng Meyer) and ginsenoside Rg5. J Ginseng Res 2015;39:125–34.

[11] Oh J, Yoon HJ, Jang JH, Kim DH, Surh YJ. The standardized Korean Red Ginseng extract and its ingredient ginsenoside Rg3 inhibit manifestation of breast cancer stem cell-like properties through modulation of self-renewal signaling. J Ginseng Res 2019;43:421–30.

[12] Pietenpol JA, Stewart ZA. Cell cycle checkpoint signaling: cell cycle arrest versus apoptosis. Toxicology 2002;181–182:475–81.

[13] Musacchio A, Salmon ED. The spindle-assembly checkpoint in space and time. Nat Rev Mol Cell Biol 2007;8:379–93.

[14] Vernos I. The chromosomal passenger complex takes center stage during mitosis. Dev Cell 2004;7:145–6.

[15] Ruchaud S, Carmena M, Earnshaw WC. Chromosomal passengers: conducting cell division. Nat Rev Mol Cell Biol 2007;8:798–812.

[16] Kim S, Kim NH, Park JE, Hwang JW, Myung N, Hwang KT, Kim YA, Jang CY, Kim YK. PRMT6-mediated H3R2me2a guides Aurora B to chromosome arms for proper chromosome segregation. Nat Commun 2020;11:612.

[17] Carmena M, Wheelock M, Funabiki H, Earnshaw WC. The chromosomal passenger complex (CPC): from easy rider to the godfather of mitosis. Nat Rev Mol Cell Biol 2012;13:789–803.

[18] Wilkins BJ, Rall NA, Ostwal Y, Kruitwagen T, Hiragami-Hamada K, Winkler M, Barral Y, Fischle W, Neumann H. A cascade of histone modifications induces chromatin condensation in mitosis. Science 2014;343:77–80.

[19] Tanno Y, Kitajima TS, Honda T, Ando Y, Ishiguro K, Watanabe Y. Phosphorylation of mammalian Sgo2 by Aurora B recruits PP2A and MCAK to centromeres. Gene Dev 2010;24:2169–79.

[20] Minoshima Y, Kawashima T, Hirose K, Tonozuka Y, Kawajiri A, Bao YC, Deng X, Tatsuka M, Narumiya S, May Jr WS, Nosaka T, Semba K, Inoue T, Satoh T, Inagaki M, Kitamura T. Phosphorylation by aurora B converts MgcRacGAP to a RhoGAP during cytokinesis. Dev Cell 2003;4:549–60.

[21] Ng WY, Chao CY. Effects of ginsenosides Rg1 and Rb1 of Panax ginseng on mitosis in root tip cells of Allium cepa. Am J Chin Med 1981;9:119–33.

[22] Huang J, Li LS, Yang DL, Gong QH, Deng J, Huang XN. Inhibitory effect of ginsenoside Rg1 on vascular smooth muscle cell proliferation induced by PDGF-BB is involved in nitric oxide formation. Evid-Based Compl Alt 2012;2012.

[23] Li SG, Yan MZ, Zhang D, Ye M, Deng JJ. Effects of ginsenoside Rg1 on the senescence of vascular smooth muscle cells. Genet Mol Res 2016;15.

[24] Tang YL, Zhang CG, Liu H, Zhou Y, Wang YP, Li Y, Han YJ, Wang CL. Ginsenoside Rg1 inhibits cell proliferation and induces markers of cell senescence in CD34+CD38- leukemia stem cells derived from KG1alpha acute myeloid leukemia cells by activating the Sirtuin 1 (SIRT1)/Tuberous Sclerosis complex 2 (TSC2) signaling pathway. Med Sci Mon Int Med J Exp Clin Res 2020;26: e918207.

[25] Méndez J, Stillman B. Chromatin association of human origin recognition complex, cdc6, and minichromosome maintenance proteins during the cell cycle: assembly of prereplication complexes in late mitosis. Mol Cell Biol 2000;20:8602–12.

[26] Yi Q, Chen QF, Yan HY, Zhang M, Liang C, Xiang XF, Pan X, Wang FW. Aurora B kinase activity-dependent and -independent functions of the chromosomal passenger complex in regulating sister chromatid cohesion. J Biol Chem 2019;294:2021–35.

[27] Knowlton AL, Lan WJ, Stukenberg PT. Aurora B is enriched at merotelic attachment sites, where it regulates MCAK. Curr Biol 2006;16:1705–10.

[28] Kelly AE, Ghenoiu C, Xue JZ, Zierhut C, Kimura H, Funabiki H. Survivin reads phosphorylated histone H3 threonine 3 to activate the mitotic kinase Aurora B. Science 2010;330:235–9.

[29] Wang FW, Dai J, Daum JR, Niedzialkowska E, Banerjee B, Stukenberg PT, Gorbsky GJ, Higgins JMG. Histone H3 Thr-3 phosphorylation by Haspin positions aurora B at centromeres in mitosis. Science 2010;330:231–5.

[30] Kawashima SA, Yamagishi Y, Honda T, Ishiguro K, Watanabe Y. Phosphorylation of H2A by Bub1 prevents chromosomal instability through localizing Shugoshin. Science 2010;327:172–7.

[31] Zou M, Wang J, Gao J, Han H, Fang Y. Phosphoproteomic analysis of the antitumor effects of ginsenoside Rg3 in human breast cancer cells. Oncol Lett 2018;15:2889–98.

[32] Chen Z, Wei X, Shen L, Zhu H, Zheng X. 20(S)-ginsenoside-Rg3 reverses temozolomide resistance and restrains epithelial-mesenchymal transition progression in glioblastoma. Cancer Sci 2019;110:389–400.

[33] Sun MY, Song YN, Zhang M, Zhang CY, Zhang LJ, Zhang H. Ginsenoside Rg3 inhibits the migration and invasion of liver cancer cells by increasing the protein expression of ARHGAP9. Oncol Lett 2019;17:965–73.

[34] Wang JJ, Tian LL, Khan MN, Zhang L, Chen Q, Zhao Y, Yan Q, Fu L, Liu JW. Ginsenoside Rg3 sensitizes hypoxic lung cancer cells to cisplatin via blocking of NF-kappa B mediated epithelial-mesenchymal transition and sternness. Cancer Lett 2018;415:73–85.

[35] Xiao MH, Xia JY, Wang ZL, Hu WX, Fan YL, Jia DY, Li J, Jing PW, Wang L, Wang YP. Ginsenoside Rg1 attenuates liver injury induced by D-galactose in mice. Exp Ther Med 2018;16:4100–6.

[36] Zhou L, Tian X, Zhu C, Wang F, Higgins JM. Polo-like kinase-1 triggers histone phosphorylation by Haspin in mitosis. EMBO Rep 2014;15:273–81.

[37] Zhou L, Liang C, Chen Q, Zhang Z, Zhang B, Yan H, Qi F, Zhang M, Yi Q, Guan Y, Xiang X, Zhang X, Ye S, Wang F. The N-terminal non-kinase-domain-mediated binding of Haspin to Pds5B protects centromeric cohesion in mitosis. Curr Biol 2017;27:992–1004.

[38] Losada A, Yokochi T, Hirano T. Functional contribution of Pds5 to cohesin-mediated cohesion in human cells and Xenopus egg extracts. J Cell Sci 2005;118:2133–41.

[39] Kitajima TS, Sakuno T, Ishiguro K, Iemura S, Natsume T, Kawashima SA, Watanabe Y. Shugoshin collaborates with protein phosphatase 2A to protect cohesin. Nature 2006;441:46–52.

[40] Lee NR, Kim HS, Kim YS, Kwon MH, Choi KS, Lee CW. Regulation of the subcellular shuttling of Sgo1 between centromeres and chromosome arms by Aurora B-mediated phosphorylation. Biochem Biophys Res Commun 2014;454:429–35.

[41] van der Waal MS, Saurin AT, Vromans MJM, Vleugel M, Wurzenberger C, Gerlich DW, Medema RH, Kops GJPL, Lens SMA. Mps1 promotes rapid centromere accumulation of Aurora B. EMBO Rep 2012;13:847–54.